

Energy spectrum and the mass gap from nonperturbative quantization à la Heisenberg

Vladimir Dzhunushaliev^{1,2,3,4,*} and Vladimir Folomeev^{2,3,†}

¹ *Department of Theoretical and Nuclear Physics,*

Al-Farabi Kazakh National University, Almaty 050040, Kazakhstan

² *Institute of Experimental and Theoretical Physics,*

Al-Farabi Kazakh National University, Almaty 050040, Kazakhstan

³ *Institute of Physicotechnical Problems and Material Science of the NAS
of the Kyrgyz Republic, 265 a, Chui Street, Bishkek 720071, Kyrgyzstan*

⁴ *Institute of Systems Science, Durban University of Technology, P. O. Box 1334, Durban 4000, South Africa*

Using approximate methods of nonperturbative quantization à la Heisenberg and taking into account the interaction of gauge fields with quarks, we find regular solutions describing the following configurations: (i) a spinball consisting of two virtual quarks with opposite spins; (ii) a quantum monopole; (iii) a spinball-plus-quantum-monopole system; and (iv) a spinball-plus-quantum-dyon system. All these objects (except the spinball) are embedded in a bag created by the quantum coset condensate consisting of the $SU(3)/(SU(2) \times U(1))$ gauge fields. The existence of these objects is due to the Meissner effect, which implies that the $SU(2) \times U(1)$ gauge fields are expelled from the condensate. The physical interpretation of these solutions is proposed in two different forms: (i) an approximate glueball model; and (ii) quantum fluctuations in the coset condensate of the nonperturbative vacuum or in a quark-gluon plasma. For the spinball and the spinball-plus-quantum-monopole configuration, we obtain energy spectra, in which mass gaps are present. The process of deconfinement is discussed qualitatively. It is shown that the quantum chromodynamics constant Λ_{QCD} appears in the nonperturbative quantization à la Heisenberg as some constant controlling the correlation length of quantum fields in a spacelike direction.

PACS numbers: 12.38.Lg; 12.90.+b; 11.15.Tk

Keywords: Nonperturbative quantization, energy spectrum, mass gap, quantum dyon, quantum monopole, quarks, condensate

I. INTRODUCTION

In quantum chromodynamics (QCD), there is a consensus that the structure of the QCD vacuum is much more complicated than that of quantum electrodynamics. It is generally believed that quantum fluctuations having the form of a monopole (a hedgehog) do exist in the QCD vacuum. But the radial magnetic field of a monopole in the QCD vacuum decreases asymptotically according to an exponential law, unlike the magnetic field of the 't Hooft-Polyakov monopole which decreases according to a power law. This is a crucial distinction, leading to the problem of obtaining a monopole with a magnetic field that decays exponentially at infinity (a hedgehog).

Here, we employ a nonperturbative quantization method à la Heisenberg and its three-equation approximation for obtaining a set of equations describing a quantum monopole/dyon interacting with virtual quarks and having the required asymptotic behavior. We also show that in such system there exist solutions describing (i) virtual quarks (a spinball); (ii) a quantum monopole; (iii) a spinball-plus-quantum-monopole configuration; and (iv) a spinball-plus-quantum-dyon system, and the configurations (ii)-(iv) are enclosed within a bag. Also, in the systems (ii)-(iv), there takes place the Meissner effect: color magnetic and electric fields are expelled by the condensate created by the $SU(3)/(SU(2) \times U(1))$ gauge fields.

At the present time, there is a universally accepted point of view according to which the vacuum in gluodynamics and chromodynamics is described fairly well in the form of a dual superconductor. This idea was suggested by 't Hooft and Mandelstam in Ref. [1]. As of now, there is no any strict analytic proof of this assumption. Numerous lattice calculations provide support for that hypothesis (see, for example, Refs. [2, 3]). In Refs. [4, 5], the dual superconductivity of the ground state of $SU(2)$ gauge theory is studied in connection with confinement. The investigation of the confining properties of the QCD vacuum of dynamical quarks has been carried out in Ref. [6]. The dual

*Electronic address: v.dzhunushaliev@gmail.com

†Electronic address: vfolomeev@mail.ru

superconductivity model for confinement in QCD is discussed in detail in Ref. [7]. The progress in a gauge-invariant understanding of quark confinement based on the dual superconductivity in Yang-Mills theory is discussed in Ref. [8].

In the present paper we study configurations consisting of a quantum monopole (or a dyon) and virtual quarks embedded in a condensate supported by the $SU(3)/(SU(2) \times U(1))$ gauge fields. The condensate creates a bag within which a quantum monopole (or a dyon) is located. This means that we are dealing with the Meissner effect: the condensate [supported by the gauge coset fields $A_\mu^m \in SU(3) / (SU(2) \times U(1))$] expels the quantum dyon/monopole created by the $A_\mu^a \in SU(2) \times U(1) \subset SU(3)$ fields. To describe such systems, we use the three-equation approximation of Ref. [9] when the right-hand sides of these equations contain sources in the form of a spinor (quark) field for which there is the corresponding nonlinear Dirac equation. The three-equation approximation is the practical realization of the nonperturbative quantization method suggested by W. Heisenberg in Ref. [10]. He used this approach to describe the properties of an electron employing some fundamental equation, which he suggested to be the nonlinear Dirac equation. Within this direction, the energy spectrum of spherically symmetric configurations has been obtained in Refs. [11, 12], whose analysis showed the presence of a mass gap. Apparently, the mass gap was first obtained in the theoretical computations of Refs. [11, 12].

The paper is organized as follows. In Sec. II we present the three-equation approximation to describe the system consisting of virtual quarks, color non-Abelian gauge fields, and the condensate. In Sec. III we choose the stationary ansatz to solve the equations of Sec. II, using which the corresponding complete set of equations is written down. For this set, we seek regular solutions describing three special cases where there present either only quarks (a spinball, Sec. III A), or a color magnetic field and the condensate (a quantum monopole, Sec. III B), or a color magnetic field, the condensate, and quarks (a spinball-plus-quantum-monopole system, Sec. III C). Also, we obtain regular solutions for the general case where one has color electric and magnetic fields, the condensate, and quarks (a spinball-plus-quantum-dyon system, Sec. III D). In Sec. IV we find energy spectra for the spinball (Sec. IV A) and for the spinball-plus-quantum-monopole system (Sec. IV B), using which we show the existence of mass gaps for these spectra. In Sec. V we give a qualitative discussion of the deconfinement mechanism for the spinball and for the spinball-plus-quantum-monopole system when the nonperturbative effects are taken into account. In Sec. VI we discuss the issue of the appearance of the constant Λ_{QCD} in QCD from using the nonperturbative approach à la Heisenberg. Finally, in Sec. VII, we summarize the obtained results and give a word about possible physical applications of the systems under consideration.

II. THREE-EQUATION APPROXIMATION WITH QUARKS

Three-equation approximation has the following form (for a detailed discussion, see Ref. [9]):

$$D_\nu F^{a\mu\nu} - \left[(m^2)^{ab\mu\nu} - (\mu^2)^{ab\mu\nu} \right] A_\nu^b = \frac{g\hbar c}{2} \langle \hat{\psi} \gamma^\mu \lambda^a \hat{\psi} \rangle, \quad (1)$$

$$\langle \hat{A}_\mu^m(y) D_\nu \hat{F}^{m\mu\nu}(x) \rangle = \frac{g\hbar c}{2} \langle \hat{A}_\mu^m(y) \hat{\psi}(x) \gamma^\mu \lambda^m \hat{\psi}(x) \rangle, \quad (2)$$

$$\left\langle \hat{\psi}_{i\alpha}(y) \left\{ i\hbar \gamma^\mu \left[\partial_\mu \hat{\psi}(x) - i \frac{g}{2} \lambda^B \hat{A}_\mu^B(x) \hat{\psi}(x) \right] - m_q c \hat{\psi}(x) \right\}_{j\beta} \right\rangle = 0, \quad (3)$$

where $i, j = \{\text{red, green, blue}\}$ are the color indices of quarks; α, β are the spinor indices of quarks; g is the coupling constant; m_q is the quark mass; D_ν is the gauge derivative of the subgroup $SU(2) \times U(1)$; $(m^2)^{ab\mu\nu}$, $(\mu^2)^{ab\mu\nu}$, and $(m_\phi^2)^{ab\mu\nu}$ [see below in Eq. (6)] are quantum corrections coming from the dispersions of the operators $\widehat{\delta A}^{a\mu}$ and $\hat{A}^{m\mu}$,

$$\hat{A}^{a\mu} = \langle \hat{A}^{a\mu} \rangle + i \widehat{\delta A}^{a\mu}, \quad (4)$$

$$\langle \hat{A}^{m\mu} \rangle = 0, \quad (5)$$

where $\langle \dots \rangle$ denotes the quantum average over some nonperturbative quantum state; a is the index of the $SU(2) \times U(1) \subset SU(3)$ subgroup; λ^B are the Gell-Mann matrices; $B = 1, 2, \dots, 8$ is the index of the $SU(3)$ group. The dispersions of the quantities in Eqs. (4) and (5) are defined in Sec. VI by the formulae (71) and (72). The notion of the nonperturbative quantum state is discussed in detail in Ref. [13].

The left-hand side of Eq. (2) is derived in analogy with obtaining this equation with zero right-hand side in Ref. [9]:

$$\langle \hat{A}_\mu^m(y) D_\nu \hat{F}^{m\mu\nu}(x) \rangle = \phi(y) \left[\square \phi - (m_\phi^2)^{ab\mu\nu} A_\nu^a A_\mu^b \phi - \lambda \phi (M^2 - \phi^2) \right]. \quad (6)$$

Using the method developed in [9], one then can obtain Eq. (2).

To estimate the right-hand sides of Eqs. (1)-(3), we use approximations according to which

$$\langle \hat{\psi} \rangle = 0, \quad (7)$$

$$\langle \hat{\psi} \gamma^\mu \lambda^a \hat{\psi} \rangle = \bar{\zeta} \gamma^\mu \lambda^a \zeta, \quad (8)$$

$$\langle \hat{\psi}_{i\alpha}(y) \lambda_{jk}^m (\gamma^\mu)_{\beta\gamma} \hat{A}_\mu^m(y) \hat{\psi}_{\gamma k} \rangle = ? \quad (9)$$

Here ζ is the spinor describing the dispersion (8) of the quantum field $\hat{\psi}$ which has a zero average value (7). In this sense we consider virtual quarks for which the quantum average of $\hat{\psi}$ is equal to zero.

The relation (9), using Eq. (5), is of most interest. Let us consider the Green function (9) in more detail:

$$G_{\alpha\beta ij}(y, y, x) = \langle \hat{\psi}_{\alpha i}(y) (\lambda^m)_{jk} (\gamma^\mu)_{\beta\gamma} \hat{A}_\mu^m(y) \hat{\psi}_{\gamma k}(x) \rangle. \quad (10)$$

Here α, β, γ are the spinor indices and $i, j, k = 1, 2, 3$ (or $i, j, k = \{\text{red, green, blue}\}$) are the quark indices. One of our main purposes is to obtain an approximate expression for the Green function $G_{\alpha\beta ij}$. This function has the indices α, β and i, j , and, hence, our approximation must also have the same indices. For this purpose, we will use the dispersion of the spinor field ζ_α and the dispersion of the coset gauge field ϕ . One can construct several different variants to approximate the Green function $G_{\alpha\beta ij}$ from (10). The following approximation will be the simplest one:

$$G_{\alpha\beta ij}(y, x, x) \approx \Lambda_1 [\bar{\zeta}_{\alpha i}(y) \zeta_{\beta j}(x)] [\bar{\zeta}_{k\gamma}(x) \zeta_{k\gamma}(x)] \phi(x) = \Lambda_1 [\bar{\zeta}_{\alpha i}(y) \zeta_{\beta j}(x)] (\bar{\zeta} \zeta) \phi(x), \quad (11)$$

$$G_{\alpha\alpha ii}(x, y, x) \approx \Lambda_2 [\bar{\zeta}_{\alpha i}(y) \zeta_{\alpha i}(x)] [\bar{\zeta}_{k\gamma}(x) \zeta_{k\gamma}(x)] \phi(y) = \Lambda_2 (\bar{\zeta} \zeta)^2 \phi(y). \quad (12)$$

Here $\Lambda_{1,2}$ are some numerical coefficients. The approximation (11) is substituted into Eq. (3); cancelling $\bar{\zeta}_{\alpha i}(y)$, we obtain the nonlinear Dirac equation (15) for ζ . The approximation (12) is substituted into the right-hand side of Eq. (2); cancelling $\phi(y)$, we obtain Eq. (14) for the condensate ϕ . Physically, this approximation means that the Green function $G_{\alpha\beta ij}$, describing the correlation between quantum fluctuations of the fields \hat{A}_μ^m and $\hat{\psi}$, depends on the dispersions of quantum fluctuations of the field \hat{A}_μ^m and the quark field $\hat{\psi}$.

Hence, using the above approximations, Eqs. (1)-(3) take the final form

$$D_\nu F^{a\mu\nu} - [(m^2)^{ab\mu\nu} - (\mu^2)^{ab\mu\nu}] A_\nu^b = \frac{g\hbar c}{2} (\bar{\zeta} \gamma^\mu \lambda^a \zeta), \quad (13)$$

$$\square \phi - (m_\phi^2)^{ab\mu\nu} A_\nu^a A_\mu^b \phi - \lambda \phi (M^2 - \phi^2) = \Lambda_2 \frac{g\hbar c}{2} (\bar{\zeta} \zeta)^2, \quad (14)$$

$$i\hbar \gamma^\mu \left(\partial_\mu \zeta - i \frac{g}{2} \lambda^a A_\mu^a \zeta \right) + \Lambda_1 \frac{g\hbar}{2} \phi \zeta (\bar{\zeta} \zeta) - m_q c \zeta = 0. \quad (15)$$

III. QUANTUM DYON PLUS VIRTUAL QUARKS

We seek a solution of Eqs. (13)-(15) in the following form:

$$A_i^a = \frac{f(r) - 1}{gr^2} \epsilon_{iaj} x^j, \quad i = x, y, z \text{ (in cartesian coordinates)}, \quad (16)$$

$$A_i^a = \frac{1}{g} [1 - f(r)] \begin{pmatrix} 0 & \sin \varphi & \sin \theta \cos \theta \cos \varphi \\ 0 & -\cos \varphi & \sin \theta \cos \theta \sin \varphi \\ 0 & 0 & -\sin^2 \theta \end{pmatrix}, \quad i = r, \theta, \varphi \text{ (in polar coordinates)}, \quad (17)$$

$$A_t^a = 0, \quad (18)$$

$$A_t^8 = \frac{\chi(r)}{g}, \quad A_i^8 = 0, \quad (19)$$

$$\phi = \frac{\xi(r)}{g}, \quad (20)$$

$$\zeta^T = \frac{e^{-i\frac{Et}{\hbar}}}{gr\sqrt{2}} \left\{ \begin{pmatrix} 0 \\ -u \\ 0 \end{pmatrix}, \begin{pmatrix} u \\ 0 \\ 0 \end{pmatrix}, \begin{pmatrix} iv \sin \theta e^{-i\varphi} \\ -iv \cos \theta \\ 0 \end{pmatrix}, \begin{pmatrix} -iv \cos \theta \\ -iv \sin \theta e^{i\varphi} \\ 0 \end{pmatrix} \right\}. \quad (21)$$

Here ϵ_{iaj} is the completely antisymmetric Levi-Civita symbol; $a = 1, 2, 3$; $i, j = 1, 2, 3$ are the spacetime indices; the functions u and v depend on the radial coordinate r only; the ansatz (21) is taken from Refs. [15, 16]. After substituting the expressions (16)-(21) into Eqs. (13)-(15), we obtain the equations

$$-f'' + \frac{f(f^2 - 1)}{x^2} - m^2(1 - f)\tilde{\xi}^2 + \tilde{g}^2 \frac{\tilde{u}\tilde{v}}{x} = -\tilde{\mu}^2(1 - f), \quad (22)$$

$$\tilde{\chi}'' + \frac{2}{x}\tilde{\chi}' = \frac{1}{2\sqrt{3}}\tilde{g}^2 \frac{\tilde{u}^2 + \tilde{v}^2}{x^2}, \quad (23)$$

$$\tilde{\xi}'' + \frac{2}{x}\tilde{\xi}' = \tilde{\xi} \left[\frac{(1-f)^2}{2x^2} + \tilde{\lambda}(\tilde{\xi}^2 - \tilde{M}^2) \right] - \frac{\tilde{g}^2\tilde{\Lambda}}{8} \frac{(\tilde{u}^2 - \tilde{v}^2)^2}{x^4}, \quad (24)$$

$$\tilde{v}' + \frac{f\tilde{v}}{x} = \tilde{u} \left(-\tilde{m}_q + \tilde{E} + m^2\tilde{\Lambda} \frac{\tilde{u}^2 - \tilde{v}^2}{x^2} \tilde{\xi} + \frac{\tilde{\chi}}{2\sqrt{3}} \right), \quad (25)$$

$$\tilde{u}' - \frac{f\tilde{u}}{x} = \tilde{v} \left(-\tilde{m}_q - \tilde{E} + m^2\tilde{\Lambda} \frac{\tilde{u}^2 - \tilde{v}^2}{x^2} \tilde{\xi} - \frac{\tilde{\chi}}{2\sqrt{3}} \right). \quad (26)$$

In these equations, the following dimensionless variables are used: $\tilde{g}^2 = g^2\hbar c$ is the dimensionless coupling constant for the SU(3) gauge field; $x = r/r_0$, where r_0 is a constant corresponding to the characteristic size of the system under consideration (in Sec. VI we will show that this parameter is related to the constant Λ_{QCD}); $\tilde{u} = \sqrt{r_0}u/g$, $\tilde{v} = \sqrt{r_0}v/g$, $\tilde{\mu} = r_0\mu$, $\tilde{\xi} = r_0\xi$, $\tilde{\chi} = r_0\chi$, $\tilde{M} = gr_0M$, $\tilde{\lambda} = \lambda/g^2$, $\tilde{m}_q = cr_0m_q/\hbar$, $\tilde{E} = r_0E/(\hbar c)$, $\tilde{\Lambda} = \Lambda/r_0^3$.

In order that these equations would be Euler-Lagrange equations it is necessary to choose the following values of the dimensionless constants: $\Lambda_1 = 2m^2\Lambda$, $\Lambda_2 = \Lambda/4$. Then the dimensionless effective Lagrangian for this set of equations is as follows:

$$\begin{aligned} \tilde{\mathcal{L}}_{\text{eff}} \equiv \mathcal{L}_{\text{eff}}/(\hbar c/r_0^4) &= \frac{1}{\tilde{g}^2} \left\{ \frac{\tilde{\chi}'^2}{2} - \left[\frac{f'^2}{x^2} + \frac{(f^2 - 1)^2}{2x^4} - \tilde{\mu}^2 \frac{(f - 1)^2}{x^2} \right] - 2m^2 \left[\tilde{\xi}'^2 + \frac{(f - 1)^2}{2x^2} \tilde{\xi}^2 + \frac{\tilde{\lambda}}{2} (\tilde{\xi}^2 - \tilde{M}^2)^2 \right] \right\} \\ &+ \frac{1}{x^2} \left[-\tilde{u}\tilde{v}' + \tilde{u}'\tilde{v} - 2f \frac{\tilde{u}\tilde{v}}{x} + m^2 \frac{\tilde{\Lambda}}{2} \tilde{\xi} \frac{(\tilde{u}^2 - \tilde{v}^2)^2}{x^2} - \tilde{m}_q (\tilde{u}^2 - \tilde{v}^2) + \tilde{E} (\tilde{u}^2 + \tilde{v}^2) + \frac{\tilde{\chi}}{2\sqrt{3}} (\tilde{u}^2 + \tilde{v}^2) \right]. \end{aligned} \quad (27)$$

Next, by definition, the energy density of the Dirac field is

$$\epsilon_D = i\hbar\bar{\zeta}\gamma^0\dot{\zeta} - L_{D\text{eff}}, \quad (28)$$

where the dot denotes differentiation with respect to time. The Lagrangian of the Dirac field $L_{D\text{eff}}$ appearing here is given by the expression from (27),

$$\begin{aligned} \tilde{L}_{D\text{eff}} &= \frac{1}{x^2} \left[-\tilde{u}\tilde{v}' + \tilde{u}'\tilde{v} - 2f \frac{\tilde{u}\tilde{v}}{x} + m^2 \frac{\tilde{\Lambda}}{2} \tilde{\xi} \frac{(\tilde{u}^2 - \tilde{v}^2)^2}{x^2} - \tilde{m}_q (\tilde{u}^2 - \tilde{v}^2) + \tilde{E} (\tilde{u}^2 + \tilde{v}^2) + \frac{\tilde{\chi}}{2\sqrt{3}} (\tilde{u}^2 + \tilde{v}^2) \right] \\ &= -m^2 \frac{\tilde{\Lambda}}{2} \tilde{\xi} \frac{(\tilde{u}^2 - \tilde{v}^2)^2}{x^4}, \end{aligned} \quad (29)$$

which is obtained using Eqs. (25) and (26). Then, using the ansatz (21), the energy density of the spinor field (28) can be found in the form

$$\tilde{\epsilon}_D = \tilde{E} \frac{\tilde{u}^2 + \tilde{v}^2}{x^2} + m^2 \frac{\tilde{\Lambda}}{2} \tilde{\xi} \frac{(\tilde{u}^2 - \tilde{v}^2)^2}{x^4}. \quad (30)$$

As a result, we get the following total energy density of the system:

$$\begin{aligned} \tilde{\epsilon} &= \frac{1}{\tilde{g}^2} \left\{ \frac{\tilde{\chi}'^2}{2} + \left[\frac{f'^2}{x^2} + \frac{(f^2 - 1)^2}{2x^4} - \tilde{\mu}^2 \frac{(f - 1)^2}{x^2} \right] + 2m^2 \left[\tilde{\xi}'^2 + \frac{(f - 1)^2}{2x^2} \tilde{\xi}^2 + \frac{\tilde{\lambda}}{2} (\tilde{\xi}^2 - \tilde{M}^2)^2 \right] \right\} \\ &+ \tilde{E} \frac{\tilde{u}^2 + \tilde{v}^2}{x^2} + m^2 \frac{\tilde{\Lambda}}{2} \tilde{\xi} \frac{(\tilde{u}^2 - \tilde{v}^2)^2}{x^4} + \tilde{\epsilon}_\infty, \end{aligned} \quad (31)$$

where the arbitrary constant $\tilde{\epsilon}_\infty$ corresponding to the energy density at infinity has been also introduced.

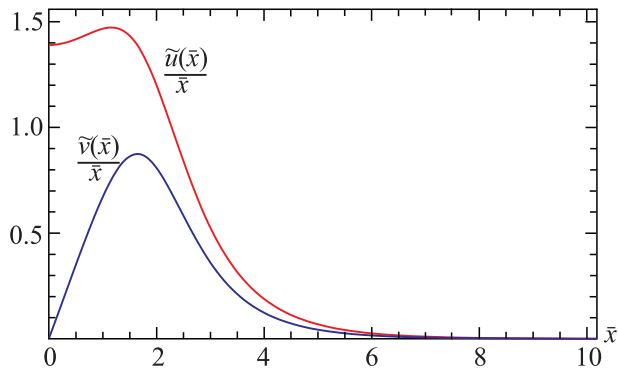


FIG. 1: The typical behavior of the solutions of Eqs. (32) and (33) describing the spinball for $\bar{\Lambda} = 1$ and $\bar{E} = 0.6$. The corresponding eigenvalue is $\tilde{u}_1 \approx 1.389621$.

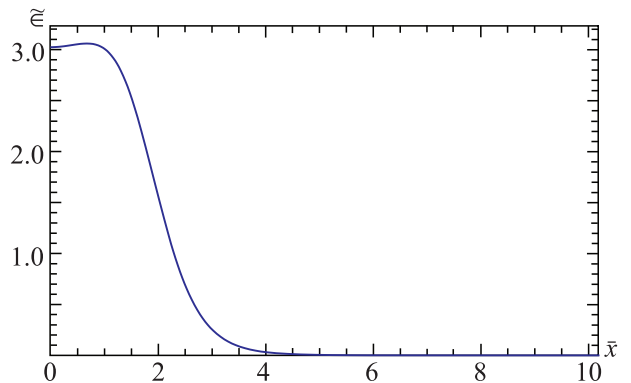


FIG. 2: The graph of the dimensionless energy density $\tilde{c}(\bar{x})/\tilde{m}_q^3$ from (37) for the spinball.

A. Spinball

Solving the complete set of equations (22)-(26) runs into great difficulty, and hence we start from considering the simplest problem without the color fields. In doing so, we assume that two virtual quarks are located at the center. Such a consideration enables one to simplify a mathematical study of the system: it allows using the ansatz employed in describing the quantum state of an electron in a hydrogen atom. Otherwise, it would be necessary to solve a problem analogous to that which occurs in describing the quantum state of two separated electrons in a helium atom.

For such a system, there are only Eqs. (25) and (26), in which we must take $f(x) = 1$ and $\tilde{\xi} = \tilde{M}$. The resulting equations are then

$$\tilde{v}' + \frac{\tilde{v}}{\bar{x}} = \tilde{u} \left(-1 + \bar{E} + \bar{\Lambda} \frac{\tilde{u}^2 - \tilde{v}^2}{\bar{x}^2} \right), \quad (32)$$

$$\tilde{u}' - \frac{\tilde{u}}{\bar{x}} = \tilde{v} \left(-1 - \bar{E} + \bar{\Lambda} \frac{\tilde{u}^2 - \tilde{v}^2}{\bar{x}^2} \right). \quad (33)$$

Here, we have introduced new dimensionless variables $\bar{x} = \tilde{m}_q x$, $\bar{E} = \tilde{E}/\tilde{m}_q$, and $\bar{\Lambda} = m^2 \tilde{m}_q \tilde{M} \tilde{\Lambda}$. Regular solutions to Eqs. (32) and (33) can be used in describing a spinball – a finite-size system consisting of two virtual quarks with opposite spins and a zero distance between them. In the neighborhood of the center of such a spinball, solutions are sought in the form

$$\tilde{u} = \tilde{u}_1 \bar{x} + \frac{\tilde{u}_3}{3!} \bar{x}^3 + \dots, \quad (34)$$

$$\tilde{v} = \frac{\tilde{v}_2}{2} \bar{x}^2 + \frac{\tilde{v}_4}{4!} \bar{x}^4 + \dots, \quad \text{where} \quad \tilde{v}_2 = \frac{2}{3} \tilde{u}_1 (-1 + \bar{E} + \bar{\Lambda} \tilde{u}_1^2). \quad (35)$$

Eqs. (32) and (33) are solved numerically as a nonlinear problem for the eigenvalue \bar{E} (or \tilde{u}_1) and the eigenfunctions $\tilde{v}(\bar{x})$ and $\tilde{u}(\bar{x})$. An example of a typical solution is shown in Fig. 1, with the asymptotic behavior

$$\tilde{u} \approx \tilde{v}_\infty e^{-\bar{x}\sqrt{1-\bar{E}^2}}, \quad \tilde{v} \approx \tilde{u}_\infty e^{-\bar{x}\sqrt{1-\bar{E}^2}}, \quad (36)$$

where \tilde{u}_∞ and \tilde{v}_∞ are integration constants.

The dimensionless energy density of the spinball under consideration can be found from Eq. (31) in the form

$$\tilde{c}(\bar{x})/\tilde{m}_q^3 = \bar{E} \frac{\tilde{u}^2 + \tilde{v}^2}{\bar{x}^2} + \frac{\bar{\Lambda}}{2} \frac{(\tilde{u}^2 - \tilde{v}^2)^2}{\bar{x}^4}. \quad (37)$$

The corresponding graph is shown in Fig. 2 for the values of the parameters of the system given in caption to Fig. 1. Note that here and in Secs. III B, III C, and III D we set $\tilde{c}_\infty = 0$.

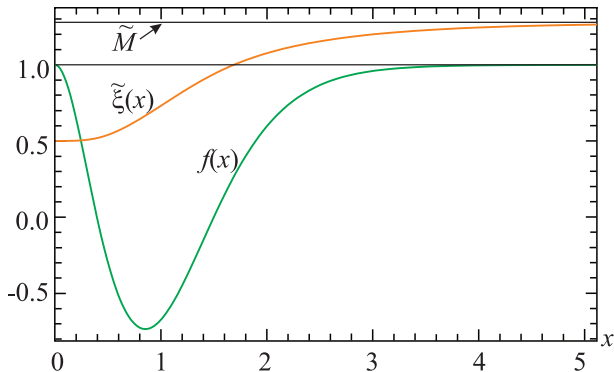


FIG. 3: The typical behavior of the functions $f(x)$ and $\tilde{\xi}(x)$ of the solution describing the quantum monopole at $f_2 = -20$, $m = 3$, $\tilde{\lambda} = 0.1$, and $\tilde{\xi}(0) = 0.5$. The corresponding eigenvalues are $\tilde{\mu} = 2.68238579$ and $\tilde{M} = 1.2786$.

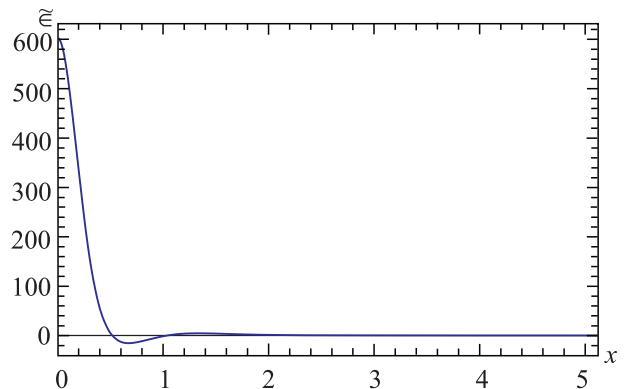


FIG. 4: The graph of the dimensionless energy density (43) of the quantum monopole.

B. Quantum monopole

In this section we consider one more simplified configuration – the quantum monopole [14]. In doing so, we will use Eqs. (22) and (24) with the color gauge field (i.e., when $f(x) \neq 1$) and without quarks (i.e., when $\tilde{v}(x) = \tilde{u}(x) = 0$):

$$-f'' + \frac{f(f^2 - 1)}{x^2} - m^2(1 - f)\tilde{\xi}^2 = -\tilde{\mu}^2(1 - f), \quad (38)$$

$$\tilde{\xi}'' + \frac{2}{x}\tilde{\xi}' = \tilde{\xi} \left[\frac{(1 - f)^2}{2x^2} + \tilde{\lambda}(\tilde{\xi}^2 - \tilde{M}^2) \right]. \quad (39)$$

We seek solutions in the neighborhood of the center in the form

$$f = 1 + \frac{f_2}{2}x^2 + \dots, \quad (40)$$

$$\tilde{\xi} = \tilde{\xi}_0 + \frac{\tilde{\xi}_2}{2}x^2 + \dots, \quad (41)$$

where the expansion coefficient f_2 is arbitrary and $\tilde{\xi}_2 = \tilde{\lambda}\tilde{\xi}_0(\tilde{\xi}_0^2 - \tilde{M}^2)/3$. Using these boundary conditions, Eqs. (38) and (39) are solved as a nonlinear problem for the eigenvalues $\tilde{M}, \tilde{\mu}$ and the eigenfunctions $\tilde{\xi}(x), f(x)$. The results of numerical calculations are given in Fig. 3. The corresponding asymptotic behavior of these solutions is as follows:

$$f(x) \approx 1 - f_\infty e^{-x\sqrt{m^2\tilde{M}^2 - \tilde{\mu}^2}}, \quad \tilde{\xi}(x) \approx \tilde{M} - \tilde{\xi}_\infty \frac{e^{-x\sqrt{2\tilde{\lambda}\tilde{M}^2}}}{x}, \quad (42)$$

where $\tilde{\xi}_\infty, f_\infty$ are integration constants. The obtained solutions describe a quantum monopole placed in the coset condensate, and such a quantum monopole is expelled from the condensate due to the Meissner effect.

The dimensionless energy density of the quantum monopole can be found from Eq. (31) in the form

$$\tilde{\epsilon} = \frac{1}{\tilde{g}^2} \left\{ \left[\frac{f'^2}{x^2} + \frac{(f^2 - 1)^2}{2x^4} - \mu^2 \frac{(f - 1)^2}{x^2} \right] + 2m^2 \left[\tilde{\xi}'^2 + \frac{(f - 1)^2}{2x^2} \tilde{\xi}^2 + \frac{\tilde{\lambda}}{2} (\tilde{\xi}^2 - \tilde{M}^2)^2 \right] \right\}. \quad (43)$$

The corresponding graph is shown in Fig. 4 for the values of the parameters of the system given in caption to Fig. 3.

Consider now the physical meaning of the parameter f_2 . Using Eq. (40), for the radial magnetic field H_r^a in the neighbourhood of the origin, one can find

$$\tilde{H}_r^{1,2,3} = \frac{1 - f^2}{x^2} \approx -f_2. \quad (44)$$

Hence f_2 gives the magnitude of the magnetic field at the center of the quantum monopole.

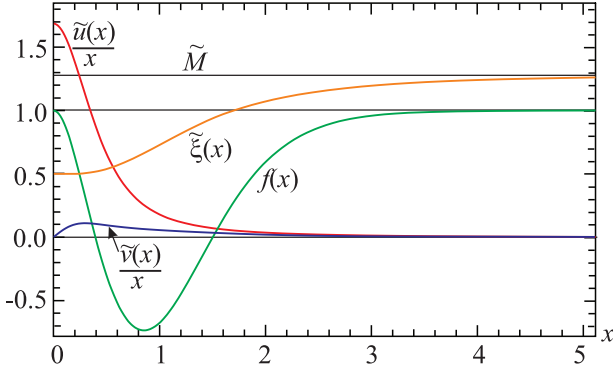


FIG. 5: The graphs of the functions $\tilde{v}(x)$, $\tilde{u}(x)$, $f(x)$, and $\tilde{\xi}(x)$ of the solution describing the spinball-plus-quantum-monopole system at $\tilde{\lambda} = 0.1$, $\tilde{\Lambda} = 1/9$, $\tilde{m}_q = 1$, $\tilde{E} = 0.8$, $m = 3$, $\tilde{g} = 1$, $\tilde{\xi}_0 = 0.5$, and $f_2 = -20$. The corresponding eigenvalues are $\tilde{\mu} \approx 2.6727842881$, $\tilde{M} \approx 1.2756$, and $\tilde{u}_1 \approx 1.68655$.

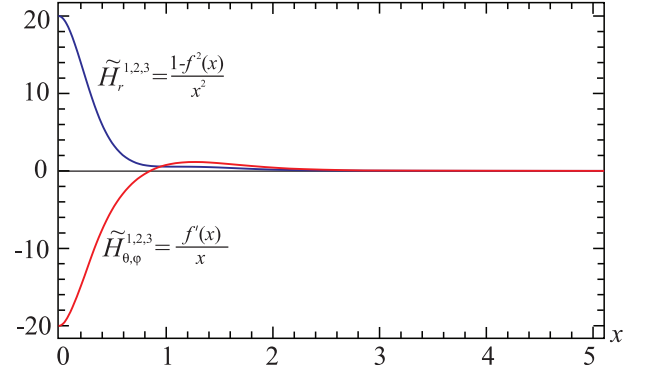


FIG. 6: The profiles of the magnetic fields $\tilde{H}_r^{1,2,3}$ and $\tilde{H}_{\theta,\varphi}^{1,2,3}$ for the spinball-plus-quantum-monopole configuration.

C. Spinball plus a quantum monopole

In this section we consider a solution of the set of equations

$$-f'' + \frac{f(f^2 - 1)}{x^2} - m^2(1 - f)\tilde{\xi}^2 + \tilde{g}^2 \frac{\tilde{u}\tilde{v}}{x} = -\tilde{\mu}^2(1 - f), \quad (45)$$

$$\tilde{\xi}'' + \frac{2}{x}\tilde{\xi}' = \tilde{\xi} \left[\frac{(1-f)^2}{2x^2} + \tilde{\lambda}(\tilde{\xi}^2 - \tilde{M}^2) \right] - \frac{\tilde{g}^2\tilde{\Lambda}}{8} \frac{(\tilde{u}^2 - \tilde{v}^2)^2}{x^4}, \quad (46)$$

$$\tilde{v}' + \frac{f\tilde{v}}{x} = \tilde{u} \left(-\tilde{m}_q + \tilde{E} + m^2\tilde{\Lambda} \frac{\tilde{u}^2 - \tilde{v}^2}{x^2} \tilde{\xi} \right), \quad (47)$$

$$\tilde{u}' - \frac{f\tilde{u}}{x} = \tilde{v} \left(-\tilde{m}_q - \tilde{E} + m^2\tilde{\Lambda} \frac{\tilde{u}^2 - \tilde{v}^2}{x^2} \tilde{\xi} \right). \quad (48)$$

These equations describe a system consisting of a quantum monopole, two virtual quarks, an extra color magnetic field created by them, and the condensate. Because of the Meissner effect, the magnetic field is expelled by the condensate creating the quantum monopole (hedgehog). The color magnetic field is produced both by the quantum monopole and by the virtual quarks. In such a configuration the virtual quarks are located at an infinitely small distance from each other that, as in Sec. III A, enables one to use for their modeling the ansatz employed in describing an electron in a hydrogen atom.

As $x \rightarrow 0$, the solution of the above set of equations can be presented in the form of the following expansions:

$$f = 1 + \frac{f_2}{2}x^2 + \dots, \quad (49)$$

$$\tilde{\xi} = \tilde{\xi}_0 + \frac{\tilde{\xi}_2}{2}x^2 + \dots, \quad (50)$$

$$\tilde{u} = \tilde{u}_1x + \frac{\tilde{u}_3}{3!}x^3 + \dots, \quad (51)$$

$$\tilde{v} = \frac{\tilde{v}_2}{2}x^2 + \frac{\tilde{v}_4}{4!}x^4 + \dots, \quad \text{where } \tilde{v}_2 = \frac{2}{3}\tilde{u}_1 \left(\tilde{E} - \tilde{m}_q + m^2\tilde{\Lambda}\tilde{\xi}_0\tilde{u}_1^2 \right). \quad (52)$$

Eqs. (45)-(48) are solved numerically as a nonlinear problem for the eigenvalues $\tilde{\mu}$, \tilde{M} , \tilde{E} and the eigenfunctions $f(x)$, $\tilde{\xi}(x)$, $\tilde{v}(x)$, $\tilde{u}(x)$. Fig. 5 shows the typical behavior of the solutions. Their asymptotic behavior as $x \rightarrow \infty$ is

$$f(x) \approx 1 - f_\infty e^{-x\sqrt{m^2\tilde{M}^2 - \tilde{\mu}^2}}, \quad \tilde{\xi}(x) \approx \tilde{M} - \tilde{\xi}_\infty \frac{e^{-x\sqrt{2\tilde{\lambda}\tilde{M}^2}}}{x}, \quad (53)$$

$$\tilde{u} \approx \tilde{u}_\infty e^{-x\sqrt{\tilde{m}_q^2 - \tilde{E}^2}}, \quad \tilde{v} \approx \tilde{v}_\infty e^{-x\sqrt{\tilde{m}_q^2 - \tilde{E}^2}}, \quad (54)$$

where $f_\infty, \tilde{\xi}_\infty, \tilde{v}_\infty$, and \tilde{u}_∞ are integration constants. The corresponding distributions of different components of the color magnetic field are shown in Fig. 6.

The dimensionless energy density of the system in question can be obtained from (31) in the form

$$\begin{aligned} \tilde{\epsilon} = \frac{1}{\tilde{g}^2} \left\{ \left[\frac{f'^2}{x^2} + \frac{(f^2 - 1)^2}{2x^4} - \tilde{\mu}^2 \frac{(f - 1)^2}{x^2} \right] + 2m^2 \left[\tilde{\xi}'^2 + \frac{(f - 1)^2}{2x^2} \tilde{\xi}^2 + \frac{\tilde{\lambda}}{2} (\tilde{\xi}^2 - \tilde{M}^2)^2 \right] \right\} \\ + \tilde{E} \frac{\tilde{u}^2 + \tilde{v}^2}{x^2} + m^2 \frac{\tilde{\Lambda}}{2} \tilde{\xi} \frac{(\tilde{u}^2 - \tilde{v}^2)^2}{x^4}. \end{aligned} \quad (55)$$

When one chooses, for instance, $f_2 = -20$ and $\tilde{E} = 0.8$, and also uses the same values of the free parameters as those for the system from Sec. III B (see in caption to Fig. 3), its graph practically coincides with that of the energy density of the quantum monopole shown in Fig. 4.

D. Spinball plus a quantum dyon

Here, we consider the complete set of equations (22)-(26) describing a quantum system with color electric and magnetic fields (a quantum dyon) plus quarks. Similarly to the previous sections, we seek a solution of these equations as $x \rightarrow 0$ in the following form:

$$f = 1 + \frac{f_2}{2}x^2 + \dots, \quad (56)$$

$$\tilde{\chi} = \tilde{\chi}_0 + \tilde{\chi}_2 \frac{x^2}{2} + \dots, \quad (57)$$

$$\tilde{\xi} = \tilde{\xi}_0 + \frac{\tilde{\xi}_2}{2}x^2 + \dots, \quad (58)$$

$$\tilde{u} = \tilde{u}_1 x + \frac{\tilde{u}_3}{3!}x^3 + \dots, \quad (59)$$

$$\tilde{v} = \frac{\tilde{v}_2}{2}x^2 + \frac{\tilde{v}_4}{4!}x^4 + \dots, \quad \text{where} \quad \tilde{v}_2 = \frac{2}{3}\tilde{u}_1 \left(\tilde{E} - \tilde{m}_q + m^2 \tilde{\Lambda} \tilde{\xi}_0 \tilde{u}_1^2 + \frac{\tilde{\chi}_0}{2\sqrt{3}} \right). \quad (60)$$

As before, Eqs. (22)-(26) are solved numerically as a nonlinear problem for the eigenvalues $\tilde{\mu}, \tilde{M}, \tilde{E}$ and the eigenfunctions $f(x), \tilde{\chi}, \tilde{\xi}(x), \tilde{v}(x), \tilde{u}(x)$. Examples of the corresponding solutions are given in Figs. 7 and 8. Their asymptotic

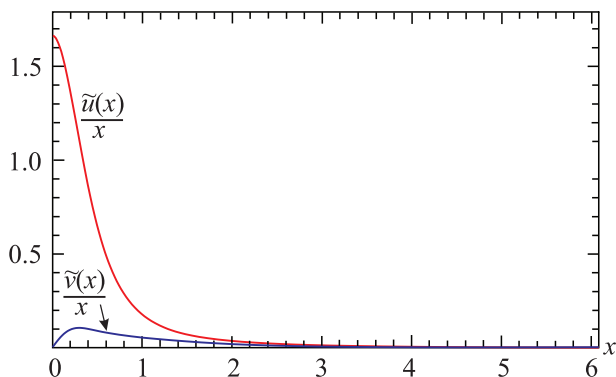


FIG. 7: The graphs of the functions $\tilde{v}(x)$ and $\tilde{u}(x)$ of the solution describing the spinball-plus-quantum-dyon system at $\tilde{\lambda} = 0.1$, $\tilde{\Lambda} = 1/9$, $\tilde{m}_q = 1$, $m = 3$, $\tilde{g} = 1$, $\tilde{\xi}_0 = 0.5$, $f_2 = -20$, $\tilde{\chi}_0 = 0$, and $\tilde{E} = 0.8$. The corresponding eigenvalues are $\tilde{M} \approx 1.275$, $\tilde{\mu} \approx 2.6725351952$, and $\tilde{u}_1 \approx 1.6653$.

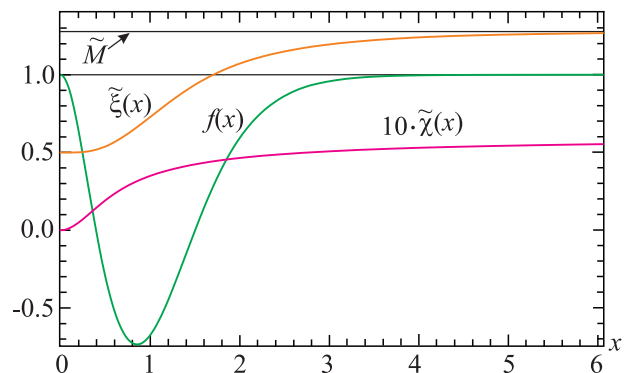


FIG. 8: The profiles of the functions $\tilde{\xi}(x), f(x)$, and $\tilde{\chi}(x)$ for the values of the parameters given in caption to Fig. 7.

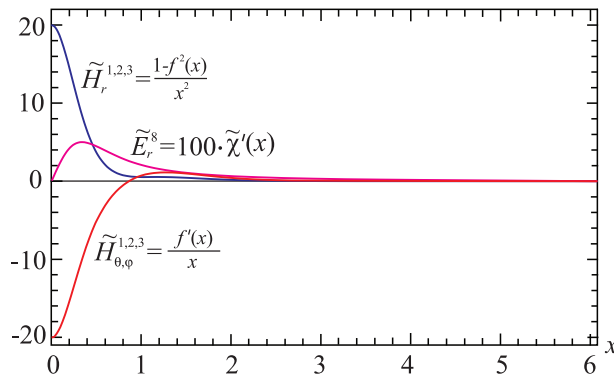


FIG. 9: The profiles of the color magnetic, $\tilde{H}_r^{1,2,3}$, $\tilde{H}_{\theta,\varphi}^{1,2,3}$, and electric, \tilde{E}_r^8 , fields for the spinball-plus-quantum-dyon configuration.

behavior as $x \rightarrow \infty$ is as follows:

$$f(x) \approx 1 - f_\infty e^{-x\sqrt{m^2\tilde{M}^2 - \tilde{\mu}^2}}, \quad \tilde{\chi}(x) \approx \tilde{\chi}_\infty - \frac{Q}{x}, \quad \tilde{\xi}(x) \approx \tilde{M} - \tilde{\xi}_\infty \frac{e^{-x\sqrt{2\tilde{\lambda}\tilde{M}^2}}}{x}, \quad (61)$$

$$\tilde{u} \approx \tilde{u}_\infty e^{-x\sqrt{\tilde{m}_q^2 - \tilde{E}^2}}, \quad \tilde{v} \approx \tilde{v}_\infty e^{-x\sqrt{\tilde{m}_q^2 - \tilde{E}^2}}. \quad (62)$$

Here f_∞ , $\tilde{\chi}_\infty$, Q , $\tilde{\xi}_\infty$, \tilde{v}_∞ , and \tilde{u}_∞ are some constants. The corresponding distributions of different components of the color magnetic and electric fields are shown in Fig. 9.

The energy density of the quantum dyon embedded in the condensate is given by the expression (31), and its graph practically coincides with that of the energy density of the quantum monopole shown in Fig. 4 (for the same values of the free parameters).

It must be emphasized here that there is a crucial difference between asymptotic behaviors of the color magnetic and electric fields (see Eq. (61) and Fig. 9): the magnetic field decreases according to an exponential law and the electric field – according to a power law (the Coulomb law).

IV. MASS GAP IN THE NONPERTURBATIVE QUANTIZATION À LA HEISENBERG

In this section we consider energy spectra of two systems (spinball and spinball-plus-quantum-monopole ones) and show the existence of mass gaps in them.

A. Mass gap for the spinball

Let us calculate an energy spectrum of the spinball described by Eqs. (32) and (33). In these equations, there is only one parameter, \bar{E} , giving the energy. Two remaining parameters ($\bar{\Lambda}$ and \bar{g}) are the constants of the theory, and they cannot change. Solving these equations for different values of the parameter \bar{E} , we get the data given in Table I. Figs. 10 and 11 show the families of the corresponding solutions for the functions $\tilde{v}(x)$ and $\tilde{u}(x)$.

\bar{E}	0.1	0.2	0.4	0.6	0.8	0.9	0.99	0.999	0.9999
\tilde{u}_1	1.103640998	1.20242169	1.34371184	1.389621	1.2745556	1.06477	0.419164	0.1366701	0.0433583
\bar{W}_t	18585	2985.04	470.563	152.677	66.4478	49.285	74.2536	213.603	668.854

TABLE I: Eigenvalues \tilde{u}_1 and the total energy \bar{W}_t from (64) as functions of the parameter \bar{E} .

The dimensionless energy density for the spinball under consideration has the following form:

$$\tilde{\epsilon}(\bar{x}) = \tilde{m}_q^3 \left[\bar{E} \frac{\tilde{u}^2 + \tilde{v}^2}{\bar{x}^2} + \frac{\bar{\Lambda}}{2} \frac{(\tilde{u}^2 - \tilde{v}^2)^2}{\bar{x}^4} \right] = \tilde{m}_q^3 \bar{\epsilon}(\bar{x}). \quad (63)$$

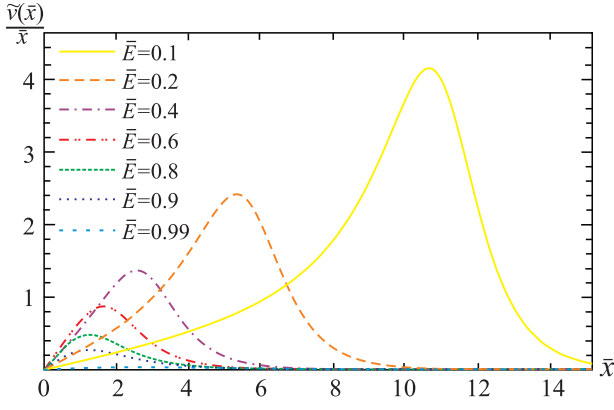


FIG. 10: Family of the spinball solutions $\tilde{v}(\bar{x})$ for different values of the parameter \bar{E} .

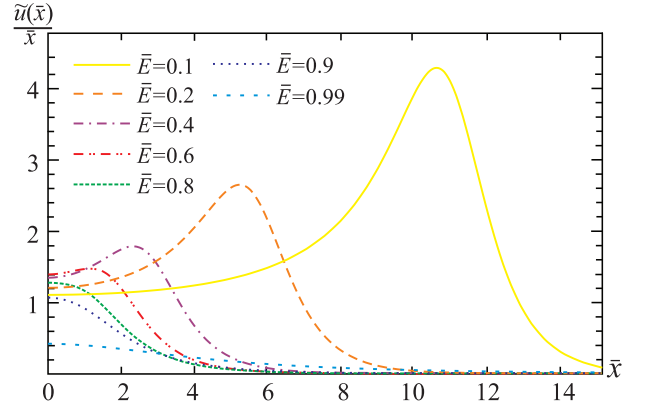


FIG. 11: Family of the spinball solutions $\tilde{u}(\bar{x})$ for different values of the parameter \bar{E} .

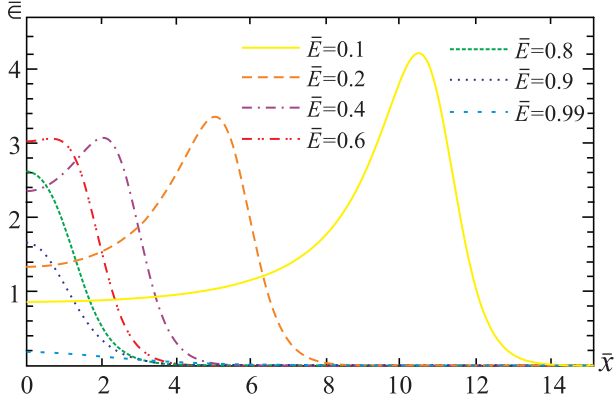


FIG. 12: Family of the spinball energy densities $\bar{\epsilon}(\bar{x})$ for different values of the parameter \bar{E} .

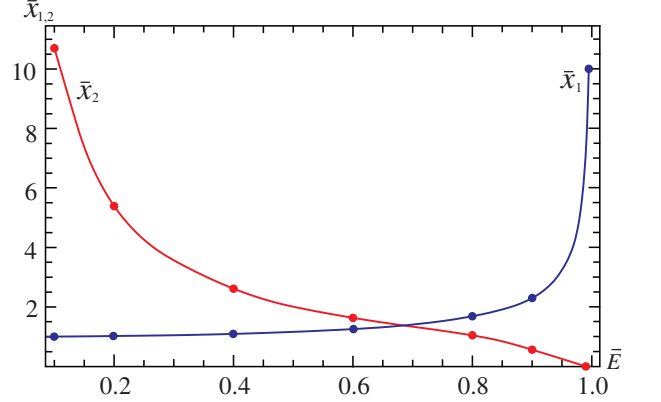


FIG. 13: The dependence of the characteristic sizes of the spinball for the left- and right-hand branches of the energy spectrum shown in Fig. 15.

The corresponding profiles of $\bar{\epsilon}(\bar{x})$ are shown in Fig. 12. The numerical analysis indicates that as $\bar{E} \rightarrow 1$ the maximum of the energy density is located at $\bar{x} = 0$ and goes to 0 (see Fig. 12), and the linear size of the configuration becomes infinitely large. In this case, according to the numerical calculations, the total energy of the spinball (64) tends to infinity. In turn, as $\bar{E} \rightarrow 0$, it seems that the maximum of the energy density goes to infinity, and the location of the maximum along the radius shifts to infinity as well. This is also approved by the results of numerical calculations of the total energy (64) given in Fig. 15.

Using Eq. (63), the total dimensionless energy \tilde{W}_t of the system under consideration can be calculated as

$$\tilde{W}_t \equiv W_t / (\hbar c / r_0) = 4\pi \tilde{m}_q^3 \int_0^\infty \bar{\epsilon} \bar{x}^2 d\bar{x} = \tilde{m}_q^3 \bar{W}_t. \quad (64)$$

The dependencies $\tilde{u}_1(\bar{E})$ and $\bar{W}_t(\bar{E})$ are given in Figs. 14 and 15. It is seen from Fig. 15 that at some value of the parameter \bar{E} there exists a minimum value of the total energy \bar{W}_t . This corresponds to the presence of the mass gap Δ for the spinball in question. Apparently, a mass gap was first found for the nonlinear Dirac equation (15) (without the condensate ϕ) in Refs. [11, 12] (in the terminology of the authors, that was “the lightest stable particle”).

B. Mass gap for the spinball-plus-quantum-monopole system

Consider now more realistic case of the spinball-plus-quantum-monopole system. This is a ball filled with spinor and color magnetic fields embedded in the condensate. Its structure is described by Eqs. (45)-(48), using which, in Sec. III C we have constructed the corresponding regular solutions. Here, we find the energy spectrum of such system and show the presence of the mass gap.

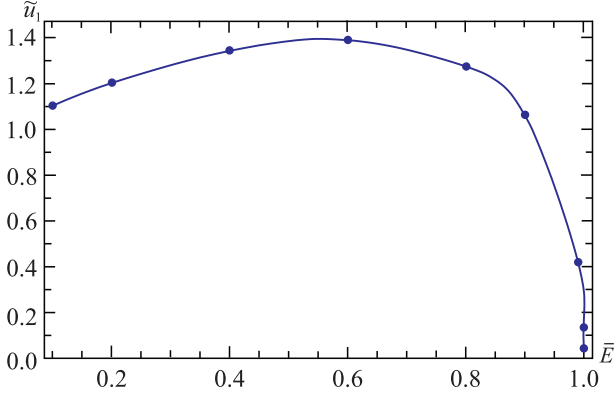


FIG. 14: The dependence of the eigenvalue \tilde{u}_1 on \bar{E} for the spinball.

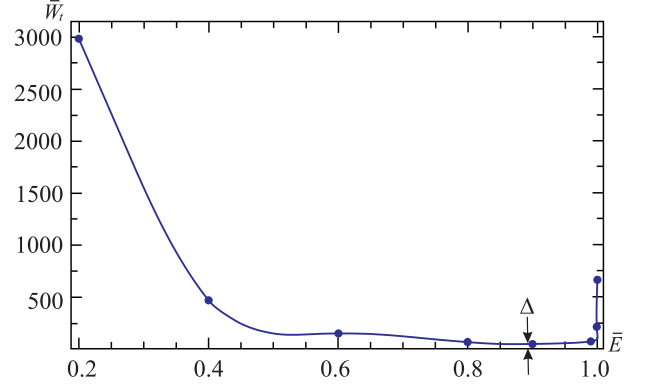


FIG. 15: The dependence of the spinball total energy \bar{W}_t on \bar{E} and the location of the mass gap Δ .

Using the expression for the dimensionless energy density $\tilde{\epsilon}$ from Eq. (55), the dimensionless total energy of the system in question is calculated as

$$\tilde{W}_t \equiv \frac{W_t}{\hbar c/r_0} = 4\pi \int_0^\infty x^2 \tilde{\epsilon} dx. \quad (65)$$

Solving the set of equations (45)-(48) numerically, we have computed this energy for different values of f_2 and \tilde{E} (see in Appendix A).

Three-dimensional and contour plots for the energy (65) are given in Figs. 16-18. Figure 17 shows the region of Fig. 16 in the vicinity of the energy minimum, i.e., the region where the mass gap is resided. One can see from this figure that there are closed lines characterising the presence of the extremum of the energy. In the case under consideration, this is the minimum corresponding to the mass gap. The approximate value of the dimensionless mass gap for the magnitudes of the parameters used here ($\tilde{\Lambda} = 1/9$, $\tilde{m}_q = 1$, $\tilde{g} = 1$, and $m = 3$) is

$$\frac{\Delta}{\hbar c/r_0} = \tilde{\Delta} \approx 32 \quad \text{at} \quad f_2 \approx -0.94, \quad \tilde{E} \approx 0.99, \quad (66)$$

where r_0 is of the order of Λ_{QCD} , as it is explained in Sec. VI.

Notice here the following important features of the system under consideration:

- The numerical analysis indicates that as $\tilde{E} \rightarrow 1$ the total energy $\tilde{W}_t \rightarrow +\infty$.
- Regular solutions to Eqs. (45)-(48) exist not for all pairs $\{f_2, \tilde{E}\}$. It is seen from Fig. 16 that for some fixed f_2 there exists a critical value \tilde{E}_{cr} at which the solution still exists but no solutions are found for $\tilde{E} < \tilde{E}_{\text{cr}}$.
- The determination of the asymptotic behavior of \tilde{W}_t as $\tilde{E} \rightarrow \tilde{E}_{\text{cr}}$ offers formidable computing difficulties. According to the numerical studies, we can assert rather confidently that in the limit $\tilde{E} \rightarrow \tilde{E}_{\text{cr}}$ the value of the total energy \tilde{W}_t (at fixed $f_2 = \text{const.}$) does not, at least, decrease, i.e., its boundary value goes either to $+\infty$ or to some constant value depending on f_2 only. As an example, Fig. 19 shows the profile of the total energy for $f_2 = -5$. It confirms that asymptotically, as $\tilde{E} \rightarrow 1$, the total energy diverges. Similar behavior of the total energy is also possible as $f_2 \rightarrow f_{2,\text{cr}}$.

Hence, one can see from the above that regular solutions to the set of equations (45)-(48) in the $\{f_2, \tilde{E}\}$ plane do exist in the region restricted by the line $\tilde{E} \rightarrow 1$ and the critical curve $\tilde{E}_{\text{cr}} = \tilde{E}_{\text{cr}}(f_2)$ (shown in Fig. 16).

V. DECONFINEMENT

In this section we give a qualitative discussion of the deconfinement mechanism when one takes into account the nonperturbative effects.

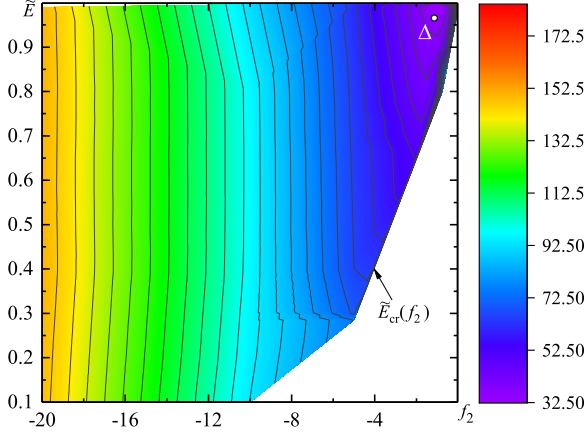


FIG. 16: Contour plot of the total energy $\tilde{W}_t(\tilde{E}, f_2)$ from Eq. (65) (the data are given in Appendix A). Δ shows the location of the mass gap in the $\{f_2, \tilde{E}\}$ plane.

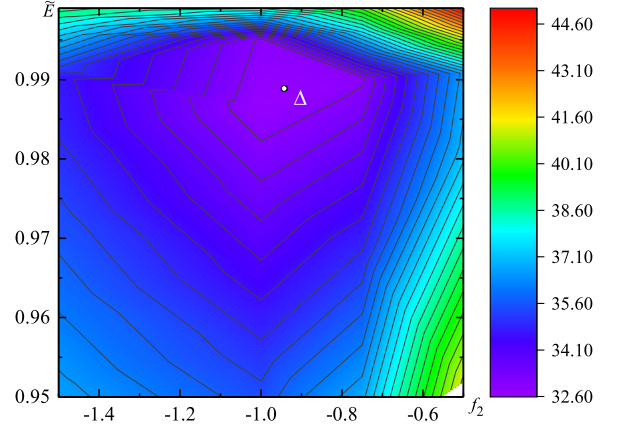


FIG. 17: Contour plot of the total energy $\tilde{W}_t(\tilde{E}, f_2)$ from Eq. (65) in the vicinity of the point where the mass gap Δ is located.

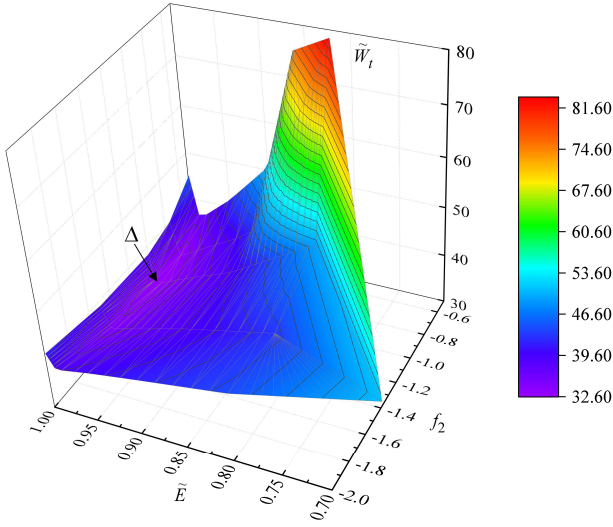


FIG. 18: Three-dimensional plot for the dependence of the total energy (65) on the parameters f_2 and \tilde{E} in the vicinity of the mass gap Δ .

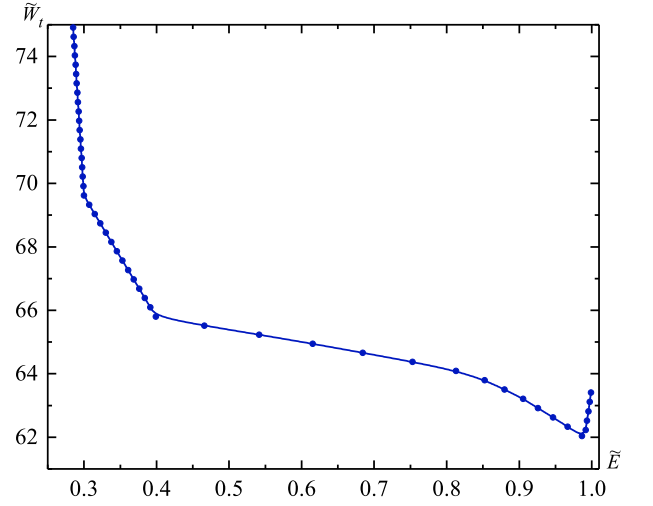


FIG. 19: The dependence of the total energy (65) on \tilde{E} at fixed $f_2 = -5$.

A. Spinball

Based on the results concerning the spinball energy spectrum obtained in Sec. IV A, it is possible to propose the following deconfinement mechanism. As is seen from Fig. 15, the energy of the spinball can be arbitrarily large. This results in the fact that with rising temperature the average energy of the spinball will increase. The typical size of the spinball for the right-hand branch of the energy spectrum, according to the asymptotic expressions (36), is defined as follows:

$$\bar{x}_1 \sim \frac{1}{\sqrt{1 - E^2}}. \quad (67)$$

It is seen from Fig. 15 that on the right-hand branch of the energy spectrum $\bar{W}_t \xrightarrow{\bar{E} \rightarrow 1} \infty$. Thus, with rising temperature, the typical size of the spinball on the right-hand branch will tend to infinity.

In turn, the typical size of the spinball \bar{x}_2 for the left-hand branch of the energy spectrum is defined as the location of maxima of the energy density given in Fig. 12. The corresponding behavior of $\bar{x}_{1,2}$ as functions of \bar{E} is shown in Fig. 13.

Given the spinball density n_s , the typical distance between spinballs is defined as follows:

$$l_s \sim (n_s)^{-1/3}. \quad (68)$$

At $\bar{x}_{1,2} \approx l_s$ the spinball solution of Sec. III A becomes incorrect. In this case quarks would not already be confined in a restricted region, and one has to consider another solution for the quarks.

Thus, one may suppose that quark deconfinement takes place at

$$\bar{x}_{1,2} \sim l_s. \quad (69)$$

Here, the typical size of the spinball depends on the temperature T . Notice that since in general case $\bar{x}_1 \neq \bar{x}_2$, deconfinement for the left- and right-hand sides of the energy spectrum will occur at different temperatures. This means that the transition from the confinement phase to the full deconfinement phase may happen in two stages. On the first stage, deconfinement occurs either for the left-hand branch or for the right-hand branch, and then deconfinement occurs for another branch of the energy spectrum.

B. Spinball plus quantum monopole

The same process will also take place for the spinball-plus-quantum-monopole configuration. According to the results obtained in Sec. IV B for the dependence of the total energy of the spinball-plus-quantum-monopole system on the parameters f_2 and \tilde{E} , the energy of such an object may also be infinite (see Figs. 16-19). In this case the typical size of the configuration is determined by the asymptotic formulae (53) and (54). One might expect that a qualitative behavior of characteristic sizes of such configurations would be similar to that of the pure spinball considered above. But this issue requires additional study that we intend to address in future work.

VI. DIMENSIONAL TRANSMUTATION, QUANTUM CORRELATORS IN A SPACELIKE DIRECTION, AND Λ_{QCD}

Let us now discuss how the constant Λ_{QCD} appears in QCD from using the nonperturbative approach à la Heisenberg. As is known, the Feynman propagator (2-point Green's function), for example, for a real scalar field, is defined as follows:

$$\Delta_F(x^\mu - y^\mu) = \left\langle T \hat{\phi}(x^\mu) \hat{\phi}(y^\mu) \right\rangle, \quad (70)$$

and it is equal to zero for spacelike directions. Within the three-equation approximation used here, we deal, for instance, with the following 2-point Green functions:

$$G^{mn\mu\nu}(y, x) = \left\langle \hat{A}^{m\mu}(y) \hat{A}^{n\nu}(x) \right\rangle \approx C^{mn\mu\nu} \phi(y) \phi(x), \quad (71)$$

$$G^{ab\mu\nu}(y, x) = \left\langle \widehat{\delta A}^{a\mu}(y) \widehat{\delta A}^{b\nu}(x) \right\rangle \approx C^{ab\mu\nu}. \quad (72)$$

Here $a, b = 1, 2, 3, 8$ and $m, n = 4, 5, 6, 7$; $C^{mn\mu\nu}$ and $C^{ab\mu\nu}$ are some numerical coefficients. These Green functions, unlike the Feynman propagator (70) for a free field, are not equal to zero for spacelike directions. In Eqs. (1) and (2), we have the following quantities:

$$(m^2)^{ab\mu\nu} = -g^2 [f^{abc} f^{cpq} G^{pq\mu\nu} - f^{amn} f^{bnp} (\eta^{\mu\nu} G^{mp\alpha}{}_{\alpha} - G^{mp\nu\mu})], \quad (73)$$

$$(\mu^2)^{ab\mu\nu} = -g^2 (f^{abc} f^{cde} G^{de\mu\nu} + \eta^{\mu\nu} f^{adc} f^{cbe} G^{de\alpha}{}_{\alpha} + f^{aec} f^{cdb} G^{ed\nu\mu}), \quad (74)$$

$$(m_\phi^2)^{ab\mu\nu} = g^2 f^{amn} f^{bnp} \frac{G^{mp\nu\mu} - \eta^{\mu\nu} G^{mp\alpha}{}_{\alpha}}{G^{mm\alpha}{}_{\alpha}}. \quad (75)$$

For these Green functions, we use the approximations

$$G^{mn\mu\nu}(y, x) \approx \Delta^{mn} \mathcal{A}^\mu \mathcal{A}^\nu \phi(y) \phi(x), \quad (76)$$

$$G^{ab\mu\nu}(y, x) \approx \Delta^{ab} \mathcal{B}^\mu \mathcal{B}^\nu, \quad (77)$$

where $\Delta^{ab}(a, b = 1, 2, 3, 8)$, $\Delta^{mn}(m, n = 4, 5, 6, 7)$ are constants and $\mathcal{A}^\mu, \mathcal{B}^\mu$ are some vectors (for details see Ref. [9]). These approximations, along with the ansatz (16)-(21), permit obtaining Eqs. (22)-(26) with the constants $\mu = \tilde{\mu}/r_0$ and $M = \tilde{M}/(gr_0)$.

The asymptotic behavior of the 2-point Green function (71) is determined by the asymptotic behavior (42) and (53) of the function $\phi(x)$ describing the condensate of the coset field $A_\mu^m \in \text{SU}(3)/(\text{SU}(2) \times \text{U}(1))$. This means that the exponential drop of this Green function is determined by the parameter r_0 . Thus we have shown that the 2-point Green function (71) refers to some dimensional quantity r_0 which has the dimensions of length. This enables one to relate this constant to the following constant known from QCD: $r_0 = \Lambda_{\text{QCD}} \approx 10^{-15}$ m.

This allows us the possibility of drawing a very important conclusion: *in quantizing strongly nonlinear fields, Green's functions for spacelike directions are not equal to zero and they are determined by some characteristic dimensional quantity.* In QCD, Λ_{QCD} is such a quantity. Apparently, such quantities are not new fundamental constants but depend on the specific form of the Lagrangian of a theory in question.

VII. PHYSICAL APPLICATIONS AND CONCLUSIONS

The physical systems considered in the present paper represent the quantum condensate, which is described by the function ϕ and contains either one [when $\tilde{\epsilon}_\infty = 0$ from Eq. (31)] or some quantity (when $\tilde{\epsilon}_\infty \neq 0$) of spinballs, quantum monopoles, spinball-plus-quantum-monopole configurations, and spinball-plus-quantum-dyon systems. In the first case, we assume that one can say about an approximate glueball model (a quantum monopole or a spinball-plus-quantum-monopole system). In the second case, it is assumed that there is an approximate description of the QCD vacuum or a quark-gluon plasma filled with quantum fluctuations, each of which is either a spinball, or a quantum monopole, or a spinball-plus-quantum-monopole system, or a spinball-plus-quantum-dyon configuration. When two quantum monopoles with opposite magnetic charges are present, they will create a monopole-antimonopole pair, similar to a Cooper pair in a superconductor. Particles in such a pair will be connected by a flux tube filled with color magnetic and electric fields. Note that within the framework of the two-equation approximation in the nonperturbative quantization à la Heisenberg one can obtain an infinitely long flux tube [14]. The obtaining a finite-length flux tube runs into great difficulty, since in this case one has to solve a nonlinear eigenvalue problem for a set of partial differential equations.

Thus, the following results have been obtained:

- The energy spectra for the spinball and for the spinball-plus-quantum-monopole system. It was shown that they possess the mass gaps.
- Within the framework of the three-equation approximation, solutions describing virtual quarks and gauge fields in a bag have been found.
- It was shown that the bags are created due to the Meissner effect, when the coset condensate expels the gauge fields.
- For the quantum-monopole/dyon systems, it was shown that color magnetic and electric fields decrease asymptotically according to exponential and power laws, respectively.
- The qualitative deconfinement model has been suggested, according to which at some temperature a characteristic size of a spinball or of a spinball-plus-quantum-monopole configuration becomes comparable to a characteristic distance between them.
- It was shown that the QCD constant Λ_{QCD} appears in the nonperturbative quantization à la Heisenberg as some constant controlling the correlation length of quantum fields in a spacelike direction.
- The nonlinear Dirac equation has been used as an approximate description of an infinite set of equations for all Green functions of the spinor equation.

It is interesting to note that in the 1950's the mass gap has in fact been found in Refs. [11, 12] in solving the nonlinear Dirac equation. However, the authors did not use such term, but said of "the lightest stable particle". Those papers were devoted to study of the nonlinear Dirac equation, and W. Heisenberg offered to use it as a fundamental equation in describing the properties of an electron. In our case, we employ that equation in describing the dispersion $\langle \hat{\psi} \hat{\psi} \rangle$ of the quark field and the correlation $\langle \hat{\psi} \hat{A}_\mu^m \hat{\psi} \rangle$ between the spinor and gauge fields having a zero quantum average: $\langle \hat{\psi} \rangle = 0$ and $\langle \hat{A}_\mu^m \rangle = 0$. To the best of our knowledge, the mass gap was first obtained in Refs. [11, 12].

Also, note that the parameters $(m^2)^{ab\mu\nu}$, $(\mu^2)^{ab\mu\nu}$, and $(m_\phi^2)^{ab\mu\nu}$ are similar to the closure parameters known in turbulence modeling as the parameters appearing when one cuts off an infinite set of equations coming from the Navier-Stokes equation in stochastic averaging [17].

In conclusion, we emphasise that the calculations performed here are only valid for a stationary case.

Acknowledgements

This work was supported by Grant No. BR05236730 in Fundamental Research in Natural Sciences by the Ministry of Education and Science of the Republic of Kazakhstan.

Appendix A: The values of the total energy \tilde{W}_t and of the eigenvalues μ, M, u_1 at different f_2, \tilde{E} for the spinball-plus-quantum-monopole system

$f_2 = -0.02$									
\tilde{E}	0.999	0.99							
\tilde{W}_t	184.244	135.626							
\tilde{M}	0.5058626	0.4969855							
\tilde{u}_1	0.1972407	0.611379							
$\tilde{\mu}$	1.511959577	1.1067708306							
$f_2 = -0.03$									
\tilde{E}	0.99								
\tilde{W}_t	128.514								
\tilde{M}	0.4974293								
\tilde{u}_1	0.6127245								
$\tilde{\mu}$	1.344502706								
$f_2 = -0.055$									
\tilde{E}	0.999	0.99	0.98						
\tilde{W}_t	119.648	107.44	100.949						
\tilde{M}	0.516196205	0.50543174	0.4936347						
\tilde{u}_1	0.243579	0.523102	0.84453462						
$\tilde{\mu}$	1.5327741656	1.51099935	1.11405352						
$f_2 = -0.1$									
\tilde{E}	0.99	0.96							
\tilde{W}_t	77.3746	85.6755							
\tilde{M}	0.521154377	0.48572							
\tilde{u}_1	0.494288	1.13951853							
$\tilde{\mu}$	1.541970066	0.3700205133							
$f_2 = -0.2$									
\tilde{E}	0.99	0.95	0.94	0.935					
\tilde{W}_t	53.4363	72.8364	75.9037	77.2632					
\tilde{M}	0.543155205	0.486725	0.4803	0.47755					
u_1	0.5185539	1.22915	1.3384	1.382189					
$\tilde{\mu}$	1.58168425006	1.28706054	0.93349082	0.65949247					
$f_2 = -0.3$									
\tilde{E}	0.99	0.95	0.92						
\tilde{W}_t	43.7621	53.2165	71.4994						
\tilde{M}	0.560506893	0.53339	0.4761						
\tilde{u}_1	0.5426051	0.986012	1.4828						
$\tilde{\mu}$	1.611834686	1.5618306	1.07601345						

$f_2 = -0.5$										
\tilde{E}	0.999	0.99	0.95	0.9	0.86					
\tilde{W}_t	45.0617	35.794	41.5654	50.5971	77.1226					
\tilde{M}	0.5911	0.58888149	0.5736	0.528397	0.45553					
\tilde{u}_1	0.4228	0.579942195	0.94907	1.354263	1.8042					
$\tilde{\mu}$	1.664592205	1.6594926345	1.63061992	1.5458587	0.611046985					
$f_2 = -0.75$										
\tilde{E}	0.999	0.99	0.95	0.9	0.8					
\tilde{W}_t	40.1438	32.7476	36.797	41.5315	83.3369					
\tilde{M}	0.6197	0.6179	0.6074	0.5844	0.4397					
\tilde{u}_1	0.46625	0.613945	0.95271	1.2634	2.01221					
$\tilde{\mu}$	1.71081065	1.70675005	1.6859686	1.6431833	0.42607975					
$f_2 = -1$										
\tilde{E}	0.999	0.995	0.99	0.95	0.9	0.8				
\tilde{W}_t	38.4915	32.8123	32.3871	35.506	38.969	49.3437				
\tilde{M}	0.6441	0.6435	0.64278	0.63455	0.61812	0.5405				
\tilde{u}_1	0.498393	0.5752465	0.63976	0.9628855	1.24783	1.757792				
$\tilde{\mu}$	1.74969239	1.748021225285	1.7462147	1.729518888	1.698292	1.549794				
$f_2 = -1.5$										
\tilde{E}	0.999	0.99	0.95	0.9	0.8					
\tilde{W}_t	39.069	34.5479	36.6868	39.0081	43.0979					
\tilde{M}	0.686	0.68492	0.6791	0.6687	0.6319					
\tilde{u}_1	0.544545	0.67777	0.98365	1.24726	1.65477					
$\tilde{\mu}$	1.814320967	1.81164013	1.799302346	1.7787229	1.7076946					
$f_2 = -2$										
\tilde{E}	0.999	0.99	0.95	0.9	0.8	0.65				
\tilde{W}_t	41.6129	38.6684	40.0291	41.4517	44.1617	51.0508				
\tilde{M}	0.7217	0.7209038	0.716345	0.70807	0.6824	0.5933				
\tilde{u}_1	0.57797	0.705655	1.001478	1.2549	1.63822	2.100448				
$\tilde{\mu}$	1.868958245	1.866712314	1.856733174	1.84002302	1.78885015	1.612653				
$f_2 = -5$										
\tilde{E}	0.999	0.99	0.95	0.9	0.85	0.8	0.6	0.4	0.3	0.285
\tilde{W}_t	63.4061	61.9859	62.5747	63.2838	63.8207	64.1784	65.0102	65.7632	69.6015	74.9163
\tilde{M}	0.8746171	0.874197172522	0.87220248	0.86875	0.86437	0.859	0.82487	0.754	0.6566	0.6051
\tilde{u}_1	0.6775593	0.7899429	1.06192505	1.29695	1.4866	1.64963	2.150675	2.518245	2.712094	2.777179
$\tilde{\mu}$	2.095709819	2.0946025448	2.0898233502	2.0821753622	2.0724943067	2.06069132	1.98759467	1.83474942	1.61102212	1.46293813
$f_2 = -10$										
\tilde{E}	0.8	0.6	0.4	0.2	0.1					
\tilde{W}_t	97.2742	97.4473	97.2636	95.5211	94.0984					
\tilde{M}	1.0367	1.02065	0.995	0.9477	0.90575					
\tilde{u}_1	1.6732	2.17354	2.5443	2.841275	2.978204					
$\tilde{\mu}$	2.323585885	2.287561159	2.22761172	2.12184476	2.0248009					
$f_2 = -20$										
\tilde{E}	0.99	0.8	0.6	0.4	0.2	0.1				
\tilde{W}_t	150.043	150.458	150.137	150.499	149.143	148.621				
\tilde{M}	1.27872	1.2756	1.26741	1.257	1.2383	1.22613				
\tilde{u}_1	0.87715	1.68655	2.19175	2.57973	2.898958	3.04085				
$\tilde{\mu}$	2.6818320333	2.6727842881	2.655017293	2.627081697	2.58528345	2.5563148				

-
- [1] S. Mandelstam, Phys. Rep., 23C (1976) 245;
G. 't Hooft, "High Energy Physics", Zichichi, Editrice Compositori, Bologna, 1976.
- [2] G. S. Bali, K. Schilling, and C. Schlichter, Phys. Rev. D **51**, 5165 (1995); [hep-lat/9409005].
- [3] M. N. Chernodub and M. I. Polikarpov, In "Cambridge 1997, Confinement, duality, and nonperturbative aspects of QCD" 387-414; [hep-th/9710205].
- [4] A. Di Giacomo, B. Lucini, L. Montesi, and G. Paffuti, Phys. Rev. D **61** (2000) 034503; [hep-lat/9906024].
- [5] A. Di Giacomo, B. Lucini, L. Montesi, and G. Paffuti, Phys. Rev. D **61**, 034504 (2000); [hep-lat/9906025].
- [6] V. G. Bornyakov *et al.* [DIK Collaboration], Phys. Rev. D **70**, 074511 (2004); [hep-lat/0310011].
- [7] G. Ripka, Lect. Notes Phys. **639**, pp.1 (2004) [hep-ph/0310102].
- [8] K. I. Kondo, S. Kato, A. Shibata, and T. Shinohara, Phys. Rept. **579**, 1 (2015) [arXiv:1409.1599 [hep-th]].
- [9] V. Dzhunushaliev, EPJ Web Conf. **138**, 02003 (2017) [arXiv:1608.05662 [hep-ph]].
- [10] W. Heisenberg, *Introduction to the unified field theory of elementary particles.*, Max - Planck - Institut für Physik und Astrophysik, Interscience Publishers London, New York, Sydney, 1966;
W. Heisenberg, Nachr. Akad. Wiss. Göttingen, N8, 111(1953);
W. Heisenberg, Zs. Naturforsch., **9a**, 292(1954);
W. Heisenberg, F. Kortel und H. Mütter, Zs. Naturforsch., **10a**, 425(1955);
W. Heisenberg, Zs. für Phys., **144**, 1(1956);
P. Askali and W. Heisenberg, Zs. Naturforsch., **12a**, 177(1957);
W. Heisenberg, Nucl. Phys., **4**, 532(1957);
W. Heisenberg, Rev. Mod. Phys., **29**, 269(1957).
- [11] R. Finkelstein, R. LeLevier, and M. Ruderman, Phys. Rev. **83**, 326 (1951).
- [12] R. Finkelstein, C. Fronsdal, and P. Kaus, Phys. Rev. **103**, 1571 (1956).
- [13] V. Dzhunushaliev, V. Folomeev, and H. Quevedo, "Nonperturbative quantization à la Heisenberg and thermodynamics of monopole configurations," arXiv:1708.06381 [hep-th].
- [14] V. Dzhunushaliev, "Quantum monopole via Heisenberg quantization," arXiv:1711.01737 [hep-ph].
- [15] X. z. Li, K. l. Wang, and J. z. Zhang, Nuovo Cim. A **75** (1983) 87.
- [16] K. l. Wang and J. z. Zhang, Nuovo Cim. A **86** (1985) 32.
- [17] D. C. Wilcox, *Turbulence Modeling for CFD*, (DCW Industries, Inc. La Canada, California, 1994).